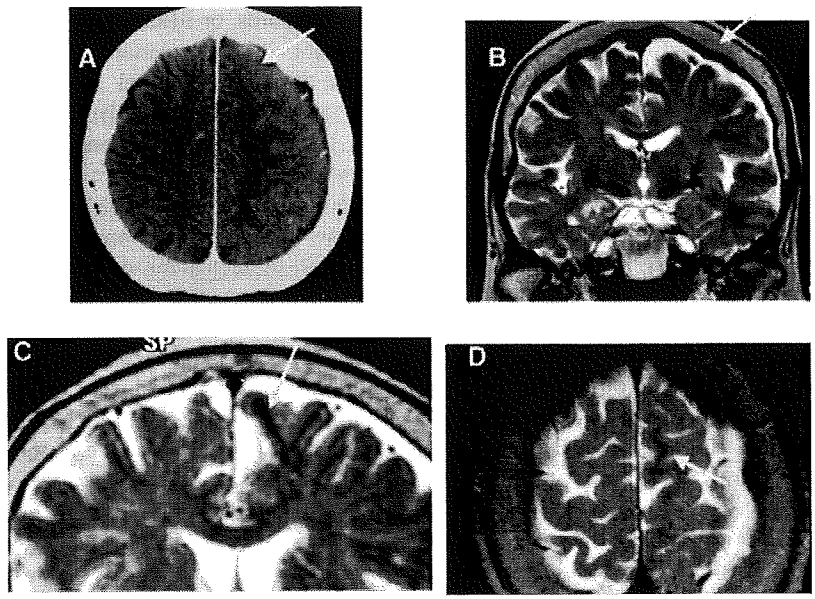

Figure 3.
An axial computed tomography (CT) (**A**) and magnetic resonance imaging (MRI) (**B–D**) of Patient 3. In the CT (A), subdural bleeding is seen as a high-density, subdural space in the left lateral convexity. It is also seen in the coronal T_2-weighted MRI as a high-intensity space in the left high lateral to mesial frontal area (**B**). T_2-weighted coronal and axial MRI (**C,D**) shows a low-intensity signal area in the mesial frontal (C) to high lateral convexity area (D), both belonging to the superior frontal gyrus around the VAC line (a line on the anterior commissure vertical to AC-PC line).

that the habitual seizure was coming. It was immediately followed by the abrupt onset of repetitive vocalization of "da-da-da-da-" for about 10 s, and then followed by complete arrest of motion and vocalization, while he was completely aware. During video-EEG monitoring, when examined by a doctor-in-charge (K.H.), both of the patient's hands could remain in the air after being passively positioned, and no apparent weakness was observed. The tonus of the all extremities was normal by neurologic examination, but he could not move all of his extremities smoothly: not at all on the right, and severely impaired on the left. When bilateral finger tapping was tested, the patient could initially execute bilaterally, but became slower bilaterally, and then stopped completely on the right and partially on the left. He could not speak out loud at all, and could not stick out his tongue. The attacks lasted for about 1 min, and then he often gave a big sigh and told us that the seizure was over. He remembered everything and knew what he was doing but could not do anything during seizures.

In Patient 2, the seizures were always preceded by a floating or rising sensation that was ill-localized within the body. It was followed by an inability to move; he could no longer write, he could not hold a pencil in his right hand and thus often dropped it, and he could not hold a cellular phone in his left hand. He could not speak out loud at all, although he knew what he wanted to say. When seizures occurred while he was standing, he could not maintain the standing posture steadily and thus stepped backward and fell on the ground. About once out of five occasions, the seizures proceeded to left hand convulsions, and then bilateral, left-side dominant, asymmetric GTCS.

In Patient 3, no auras preceded the seizures and the patient could suddenly not speak out loud at all or vocalize any words or even sounds. She had no convulsion or weakness and was aware of everything. She could communicate with hand and finger gestures, and thus the patient informed us of the beginning of an episode. At times, the family witnessed that at the beginning of event, the patient just moaned as "uh, uh, uh, uh, uh" in a rhythmic way, and then became completely mute. During the video/scalp-EEG monitoring, when the patient was examined during seizures by a doctor-in-charge (A.I.), she understood the spoken language well and thus she could follow the commands such as raising one hand and finger signs. The bilateral upper extremities showed normal tonus. She showed poor finger tapping on the right hand, and very mild proximal weakness was observed in the outstretched right arm during only several, recorded seizures. Tongue protrusion was possible but wiggling was slow.

The patient remembered the test words given during the episodes. The seizures stopped abruptly and she gave a big sigh and started talking very fluently. After the seizures, the patient clearly mentioned that she had understood the situation and what had been said to her, and she knew what she had to answer, but that she could not during seizures.

EEG findings (Table 1) and functional mapping

In Patient 1, interictal, background activity was abnormal at A and B strips due to decreased amplitude of fast activity (Fig. 4; Table 1). More than 10 habitual seizures were recorded. All the seizures started with a sharp transient and low amplitude, 100-Hz burst activity for <1 s at A2 (a posterior margin of the lesion), followed by 7–8 Hz spike activity at A2. It spread into B2 and C3-5 (a part posterior to the lesion) within 10 s (Fig. 5A, B). It then at times spread into the adjacent, lateral convexity such as E, F, and G. Clinically initial vocalization and the symptoms of NMS were observed throughout this EEG change.

For cortical stimulation with 50-Hz electric pulses, C2 showed right hand positive motor responses, most likely the SMA proper hand area. D2-D4 showed right foot positive motor responses, most likely the primary foot motor area, and D1 showed right foot sensory impairment, most likely the primary foot sensory area. However, in the rest of the electrodes, we could not increase the stimulus intensity sufficiently to examine the NMR because both mesial and lateral frontal areas were epileptically so irritable as to induce afterdischarges, simple partial seizures, or EEG seizure patterns very frequently. Therefore, it was uncertain whether NMA was present within the mesial frontal surface, mainly covered by strips of A, B, and C (Fig. 4).

In Patient 2, during video/subdural-EEG monitoring, the patient had a total of five habitual seizures (one with nonmotor symptoms and four with motor ones) (Fig. 6). At least two of the seizures were definitely preceded by very brief or ill-defined auras as described previously while the patient was lying on the bed silently, and those were immediately followed by left hand or bilateral convulsive seizures. Therefore, ictal semiologies belonging to NMS could not be examined objectively during the monitoring. In one nonmotor seizure in Fig. 7, the patient noticed the aura, and was unable to move or speak out loud at all for about 5 s, and associated ictal EEG lasted for 10 s.

In all the recorded seizures, the ictal EEG patterns started as 8–12 Hz rhythmic activities commonly at three electrodes (A6, A7, and C14) just over the cystic lesion rostral to the precentral sulcus, always before onset of tonic seizures by 4–34 s (average of 14 s) (Fig. 6). The pattern spread into the mesial and lateral sites once tonic seizures occurred. For 50-Hz cortical stimulation, six electrodes (A7, A8, C5-7, and C14), which partly included the ictal focus (A7, 8 and C14) and the adjacent, spread area (C5, 6), showed NMR involving the tongue and all extremities. Five of the six electrodes (A7, 8, C6,

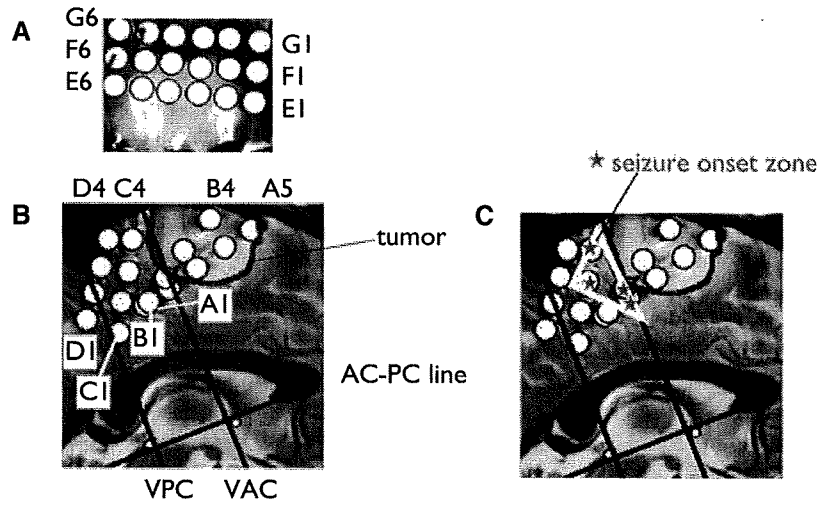

Figure 4.
Placement of subdural strip electrodes on the left lateral- (a) and mesial (b) frontal cortices in Patient 1. Strips E, F and G are placed in an anteroposterior direction with E1, F1, and G1 facing rostrally (**A**). A2 and B2 are located on the VAC line (a line on the anterior commissure vertical to AC-PC line), and the tumor is located on and anterior to the VAC line (**B**). Seizure-onset zone is labeled by asterisks at A2, B2, C3, and C4 (**C**), as also enclosed by an open triangle.

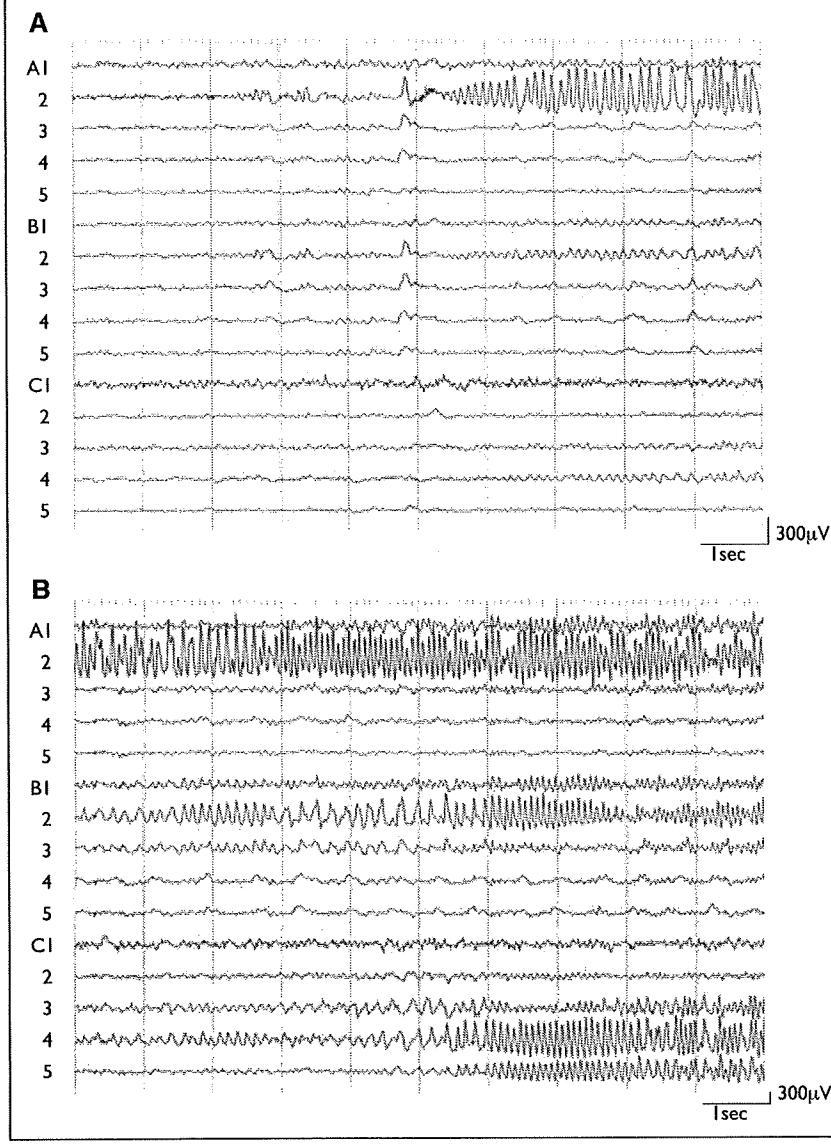

Figure 5.
Epicortical recording of ictal electroencephalography (EEG) with subdurally placed electrodes during a habitual seizure in Patient 1. All seizures started with a 100-Hz burst activity of low amplitude lasting less than 1 sec at A2, followed by 7–8 Hz spike activity at the same area (**A**). The seizure activity spread into B2, C3, and C4 within 10 s (**B**). Clinically, there was initial vocalization and then subsequent arrest of motion and vocalization were observed throughout this EEG change. *Epilepsia* © ILAE

7, and 14) also showed the habitual aura elicited by the stimulus intensity of 5–13 mA (average of 7.4 mA) (Fig. 6).

In Patient 3, routine scalp EEG revealed normal posterior dominant rhythms for her age of 77 years, and no apparent focal slow or diminished fast activity was observed. No clear epileptiform discharges were recorded during routine EEG. Prolonged video/scalp-EEG monitoring recorded small, but consistent, spikes in the vertex (maximum at Cz) during the sleep period (Fig. 8). A total of 10 seizures were recorded, and a clear ictal pattern was not specifically recorded, but questionable, low-voltage 3–6 Hz spiky activities were recorded in the vertex region (maximum at Cz). Based on those findings, it was judged that the patient had status epilepticus partialis, most likely arising from the superior frontal gyrus.

Symptoms of NMS and NMR

Commonly observed ictal semiologies among the three patients were (1) inability to speak, (2) no loss of awareness, and (3) preserved comprehension. Common findings in two patients were (1) inability to move the extremities (Patients 1 and 2), (2) normal tonus of the extremities (Patients 1 and 3), (3) indescribable or ill-localized aura (Patients 1 and 2), (4) repetitive involuntary vocalization at the beginning (Patients 1 and 3), and (5) subsequent evolution to the positive motor seizures (Patients 1 and 2). Findings observed in only one patient but clearly confirmed were (1) progressive slowing and arrest of bilateral finger movements (Patient 1), and (2) slow movements of the distal hand (Patient 3) (Table 1).

In Patient 2, cortical stimulation at the ictal focus clearly elicited NMR of the tongue and all extremities; the

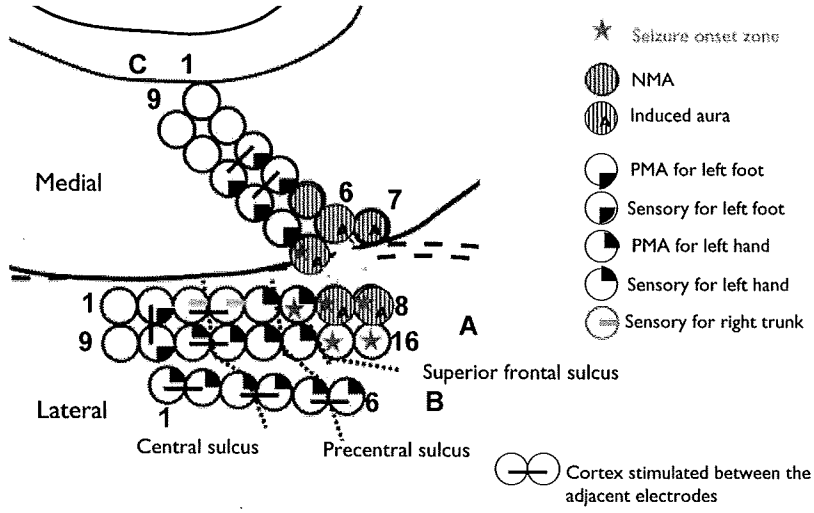

Figure 6.
Seizure-onset zone and cortical mapping in Patient 2. Ictal onset zone is defined at A6, A7, A8, A15, A16, and C14 (labeled by asterisks), and NMA at A7, A8, C5, C6, C7, and C14. Habitual auras were induced by cortical stimulation at A7, A8, C6, C7, and C14. A cystic lesion shown in Fig. 2 is present beneath A7. Pairs of adjacent electrodes connected by lines indicate cortical stimulation done between the two electrodes. Other electrodes were stimulated to a common electrode (C9). Positive cortical functions such as motor and sensory responses are shown by symbols. (NMA, negative motor area; PMA, positive motor area.)

patient could not move the tongue and all the extremities as fast as possible and then could not continue at all. All of those electrodes also elicited his habitual aura at the same time. The patient finally clearly identified that his aura corresponded exactly to the NMR. The NMR was not completely tested in Patient 1 from the seizure-onset zone because it was epileptically so irritable as to induce afterdischarges, simple partial seizures, or EEG seizure patterns very frequently.

Discussion

In the present study, we described NMS arising from the NMA that is different from focal ictal paresis, judging from the clinical semiology and its generator mechanism. It also accompanied arrest of vocalization or speech. A complex of ictal semiologies including NMS seen in the present patients was well explained by the functional anatomy of SMA proper and pre-SMA as well as the functional anatomy of lateral NMA. We also pointed out the reason that NMS was rarely observed.

Generator mechanism of NMS

In the present three patients, arrest of motion and vocalization in a conscious state was the main negative phenomena, and this clinical manifestation was very similar to NMR elicited by cortical stimulation at the NMA. Arrest of motion and vocalization could be interpreted by (1) paresis or paralysis, (2) akinesia, or (3) apraxia, occurring during an ictal period.

In the past, focal ictal paresis or paralysis was rarely described, and it was believed that loss of muscle tone with paresis, paralysis, or dropping of the affected body part was a characteristic signal (So, 1995). This ictal event was reported by several nomenclatures, as shown in Table 2. In the present three patients, decreased muscle tone was not clearly observed. When attempting to understand the difference between NMS and focal ictal paresis, it is helpful to understand the difference between epileptic interference (Penfield & Jasper, 1954) and ictal paresis. In higher cortical areas such as the speech area, epileptic activation always produces inability of the functions, for example, as in aphasia, but it never creates words or force to speak, called epileptic interference (Penfield & Rasmussen, 1950; Penfield & Jasper, 1954). NMS is regarded as epileptic interference. On the other hand, in the cortices of the fundamental functions such as primary motor or sensory areas, epileptic discharges can produce activation or inactivation (Table 3). Therefore, NMS is different from ictal paresis or paralysis, based on the viewpoint of the generator mechanism.

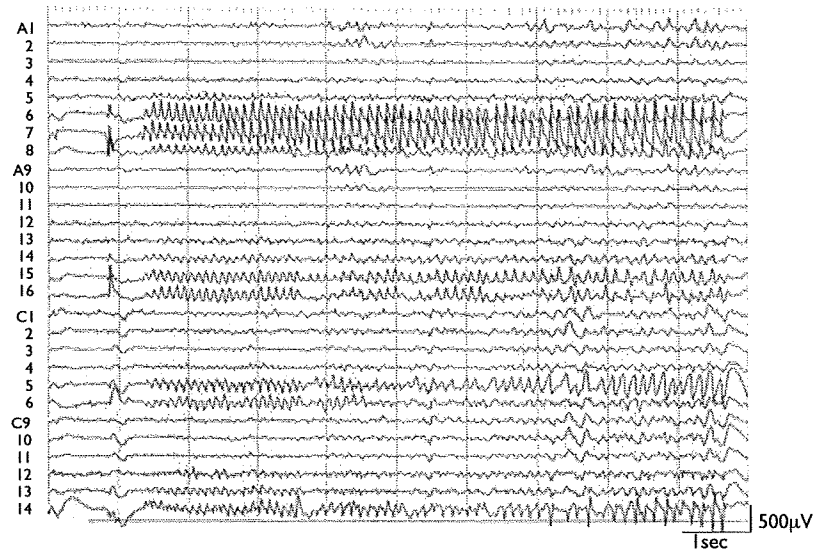

Figure 7.
Epicortical recording of ictal electroencephalography (EEG) with subdural electrodes during a habitual seizure in Patient 2. This particular seizure (only aura and nonmotor seizure) occurred when the patient was talking to the family while sitting on the bed. With the onset of the ictal pattern, the patient lay on the bed and stopped talking, and no movements were observed. Seven seconds after the end of seizure pattern, the patient quickly sat on the bed again. By the interview after the seizure, it was confirmed that the patient had a habitual aura, and could not speak or move at all immediately after the onset of aura until it had gone. All of the ictal EEG patterns started as 8–12 Hz rhythmic activities commonly involving three electrodes (A6, A7, and C14) placed rostral to the precentral sulcus just over the cystic lesion, and additionally at A8, A15, and A16 always before onset of tonic seizures by 4–34 s (average of 14 s).
Epilepsia © ILAE

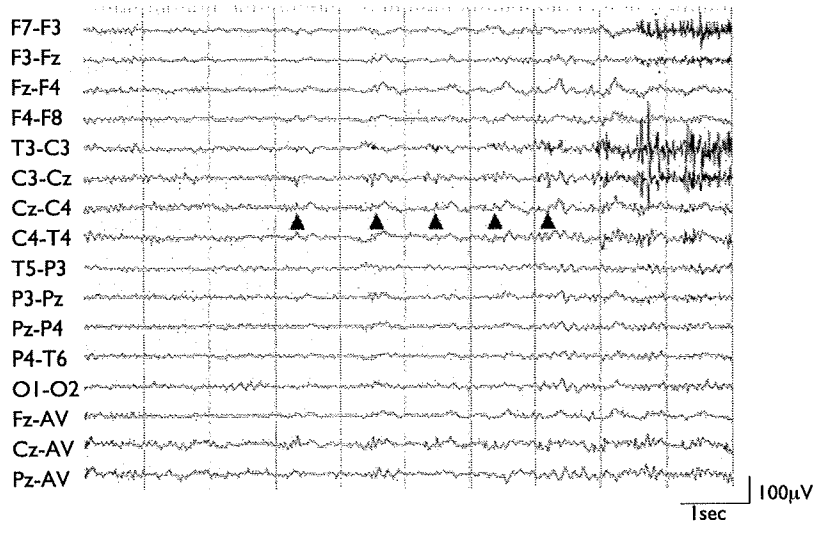

Figure 8.
Scalp-recorded interictal epileptiform discharges in Patient 3. During sleep period, the patient had small, but consistent spikes (labeled by filled triangles) at the vertex (max at Cz), which at times occurred as short runs of 3–5 s. (AV, average reference.)
Epilepsia © ILAE

In clinical neurology, the term "apraxia" is applied to a state in which a clear-minded patient with no weakness, ataxia, or other extrapyramidal derangement, and no defect of the primary modes of sensation, loses the ability to execute highly complex and previously learned skills and gestures (Ropper & Brown, 2005), and it even

Table 2. Comparison of clinical features between ictal paresis and NMS arrest of movements in the present study

	Loss of muscle tone or weakness	Ictal focus	Reference
Ictal paresis			
Ictal hemiplegia	+	SI/MI	Gowers, 1885
/monoparesis	+		Matsumoto et al., 2005
			Villani et al., 2006
Inhibitory seizures	+	SI	Abou-Khalil et al., 1995
Focal atonic/akinetic seizure	+		Gastaut & Broughton, 1972
	+	PNMA?	So, 1995
	+	NMA?	Noachtar & Lüders, 1999
NMS arrest of movements	–	Mesial premotor	Meletti et al., 2003
		NMA	The present study

PNMA, primary negative motor area; NMA, negative motor area; MI, primary motor area; SI, primary somatosensory cortex; NMS, negative motor seizure. [Correction added after online publication 20 May 2009: Ictal focus and Reference moved to top of columns]

Table 3. Comparison of proposed symptoms among epileptic interference, epileptic activation, and epileptic inactivation

Cortical areas	Epileptic interference	Epileptic activation	Epileptic inactivation
MI		Convulsion, myoclonus	Paralysis, negative myoclonus
SI		Hyperesthesia	Sensory defects
Primary visual area		Elementary visual hallucination	Scotoma
Auditory cortices		Tinnitus, auditory hallucination	Deafness
SMA proper		Tonic convulsion	Proximal
SII		Pain, hyperesthesia	weakness
Frontal eye field		Contralateral version	
Speech area	Aphasia		
SNMA (pre-SMA)	NMS	(negative myoclonus)	
PNMA (Brodmann's 44)	NMS		

MI, primary motor area; SI, primary somatosensory cortex; SMA, supplementary motor area; SII, second sensory area; SNMA, supplementary negative motor area; PNMA, primary negative motor area; NMS, negative motor seizure. [Correction added after online publication 20 May 2009: Aphasia, NMS, NMS moved under Epileptic interference column]

includes simple clumsiness. The latter can correspond to limb-kinetic apraxia. For the diagnosis of apraxia, it is important to determine whether spontaneous action or reflexive action to the unexpected stimuli is preserved, whereas praxes or skilled movements (i.e., pantomime, tool utilization, and so on) are impaired. It is not practical to check this during NMS because the seizures are rather brief, and patients may not do due to distraction by the seizures. Therefore, it may not execute suitable to call the symptoms of NMS apraxia currently. In addition, the clinical findings of apraxia are usually described in patients with chronic lesion or degenerative disorders where the compensatory restorative network system is fully employed. By contrast, in the case of symptoms of NMS, ictal activity arising from NMA can be localized at NMA or can spread to the adjacent or remote area as a dynamic ictal activity, and thus a compensatory or a modifying mechanism occurring in chronic diseases is unlikely to be present. Namely, apraxia during seizures (ictal apraxia), if present, would manifest differently than in one with chronic diseases. Therefore, the possibility that the symptoms in NMS arising from NMA are defined as apraxia could not be completely excluded. The same situation is also considered in the NMR elicited by cortical stimulation of short duration such as 5 s.

Akinesia is characterized by poverty and slowness of initiation and execution of willed and associated movements, and difficulty in changing one motor pattern to another, in the absence of paralysis (Lakke, 1981). It is usually examined by the degree of delay in the time needed to initiate a movement, as a reaction time, being regarded as an impairment of the latter phase of program of voluntary movements by the basal ganglia and its related cortical networks (Watson et al., 1992; Imai, 1996). Narabayashi (1980) described three types of akinesia: akinesia due to marked rigidity of muscles, lack of movement initiation without rigidity due to striatal dopamine deficiency, and freezing or festination in quick repetitive movements due to impairment of rhythm formation. Arrest of motion and vocalization in the present three patients might represent akinesia at least, since it is defined without weakness. However, all types of akinesia in the previous definition are related to dysfunction of the basal ganglia system and its relevant central nervous system (CNS) structures. Furthermore, symptoms of NMS and NMR (i.e., arrest of ongoing voluntary movements) develop in several seconds immediately after seizure onset and after starting cortical stimulation, respectively, but they are not the problem at the beginning like akinesia. For these two reasons, by definition, akinesia would not be appropriate to describe the symptoms of NMS. Based on the preceding discussion, it is most likely that the patients' symptoms, that is, arrest of motion and vocalization, are best defined as NMS, because there are many commonalities to the NMR.

With regard to ictal speech arrest versus aphasia, inability to speak could occur as epileptic events while the consciousness is preserved, and it is explained by motor

aphasia (ictal aphasia) (Hamilton & Matthews, 1979) or symptoms of NMS. All three patients had speech arrest, and at least two patients had arrest or slowness of tongue movements. Their comprehension was apparently preserved, and thus their speech arrest might be interpreted as simply arrest of motion or buccofacial apraxia (De Renzi et al., 1966). Because it is known that buccofacial apraxia and aphasia occur together (De Renzi et al., 1966; Kertesz & Hooper, 1982), it is possible that they occurred in our patients together. However, since the seizure focus was very limited in the several electrodes when Patients 1 and 2 had those symptoms and since the possible epileptogenic area in Patient 3 was also small as revealed by T_2-weighted image, it is unlikely that our patients had both buccofacial apraxia and aphasia, but just so-called arrest of motion, similar to NMR elicited by cortical stimulation. As discussed previously, because buccofacial apraxia was described in patients with chronic diseases, the symptoms in NMS may not be identical to buccofacial apraxia, and thus it is best to describe this ictal symptom as NMS at this time.

Location and function of NMA

Lüders et al. (1995) described the two distinct areas that produced NMR with cortical electric stimulation, that is, supplementary NMA (SNMA) and primary NMA (PNMA). SNMA was located in the rostral part of or rostral to the SMA proper, and thus at least partly it corresponded to pre-SMA in humans. PNMA was located in the posterior part of the inferior fontal gyrus, just rostral to the precentral sulcus, and thus it would be a part of the area 44 in the Brodmann's map.

In addition to those two areas, NMA was also described rostral to the precentral sulcus along it, such as in the middle frontal gyrus, and even in the lateral convexity of the superior frontal gyrus (Nii et al., 1996; Mikuni et al., 2006). In the present study, Patient 1 had ictal discharges on the mesial frontal cortex just along the line on the anterior commissure vertical to AC-PC line (VAC) and spread to the posterior part, but its anterior part was completely occupied by the tumor, and thus the pre-SMA could be dislocated posterior to it. In Patient 2, five electrodes of NMA were located in the superior frontal gyrus, but the most lateral and posterior one (A7) was located just 1–2 cm anterior to the positive motor area of the hand as shown in Fig. 2. Because the cystic lesion was present beneath or directly adjacent to the area (A7 in Fig. 6), the normal somatotopy should be distorted, and thus it is likely that the lateral NMA in Patient 2 (A7, A8 in Fig. 6) was identified as ones along the precentral sulcus in the high, lateral convexity as shown previously, being independent of pre-SMA (Nii et al., 1996; Mikuni et al., 2006). In Patient 3, since EEG and MRI both suggested abnormality in the vertex area, the symptoms were interpreted as the dysfunction of the pre-SMA.

In the recent cytoarchitectural study in animals, Matelli et al. (1991) labeled the rostral SMA as F6, which receives connection from the thalamic inputs (from the nucleus ventralis anterior and pars parvocellularis), F5 (area 44), and various prefrontal regions. F6 lacks corticospinal pathways, and those features are totally different from the caudal part of the SMA (F3 in monkeys and SMA proper in humans). F5 was defined in area 44 in the lateral frontal cortex, and it shares features similar to F3. Abundant connections from F5 to F3 have been described (Rizzolatti et al., 1988; Rizzolatti & Craighero, 2004). Because NMA is one of the most important generators of Bereitschaftspotentials (BPs) (Yazawa et al., 2000; Ikeda, 2003; Ikeda & Shibasaki, 2003; Kunieda et al., 2004), it is probably employed for the organization and integration of fine motor movements, and thus the activation of this area by high-frequency electric stimulation would produce impairment of fine movements (called "apraxia" by Lüders et al.,1995).

NMS versus NMR

A direct comparison between NMS in ictal semiology and NMR in cortical stimulation in the same patient was very difficult in the clinical documentation. In Patient 1, extensive cortical stimulation was not possible due to seizure induction; in Patient 2, NMS was too brief to be examined in detail during video-EEG monitoring. Nevertheless, as shown in the result, ictal semiologies commonly observed, at least in the two patients, are listed in the order of appearance, as (1) indescribable or ill-localized aura, (2) repetitive involuntary vocalization, (3) inability to speak, (4) inability to move the extremities, and (5) subsequent evolution to positive motor seizures. Awareness and comprehension were preserved throughout the episode before generalized seizures (Table 1). Those ictal semiologies fit well the results of cortical functional mapping made by high-frequency electric cortical stimulation including NMR. A similar, but a rather inverse sequence of ictal semiology was also reported in a patient having the mesial frontal lesion with scalp EEG and polygraphic analysis (Meletti et al., 2003).

Repetitive vocalization is often produced by high-frequency cortical stimulation in the face area in the SMA proper (Lim et al., 1994), that is, the rostral part of the SMA proper. In Patient 1, the initial ictal activity started in the mesial frontal area (A2) along the VAC line. A similar interpretation is also possible in Patient 3, even though she did not undergo invasive EEG monitoring. Because the SNMA is usually located anterior to the SMA proper, that is, anterior to the VAC line, it is conceivable that once ictal activity starts in the rostral part of the SMA proper, it then spreads further into the anterior part (pre-SMA or SNMA). In Patient 3, at the beginning of the seizures the patient had involuntary repetitive vocalization, followed

by inability to speak out and mild awkward movements of the right hand.

NMS versus ictal paresis

Focal seizures with ictal paresis or paralysis of one or more parts of the body were called focal akinetic seizures by Noachtar and Lüders, who discussed the area responsible as being in the NMA (Noachtar & Lüders, 1999). Focal akinetic seizures belongs to "inhibitory motor seizures" among focal motor seizures in the proposed international classification of epilepsy and seizures in 2001 as well as in the Report of the International League Against Epilepsy (ILAE) Classification Core Group (Engel, 2001, 2006). Recent reports have showed that focal inhibitory seizures were also associated with ictal activity in the primary motor and somatosensory cortices (Abou-Khalil et al., 1995; Matsumoto et al., 2005), that is entirely different from arrest of motion reported in the present study. The present study clearly showed that NMA is an area responsible for seizures manifesting ictal arrest of motion and vocalization, and thus we want to call it NMS, following the term of NMA.

In Patient 3, very mild weakness in the proximal part was observed in the right stretched hand during bilateral hand raising test, although not in all the seizures, but the tonus of the upper extremities was normal. It remains unresolved whether it was also explained by the ictal activity in the rostral SMA. Recently, Rubboli et al. (2006) described a so-called pure silent period in the contralateral deltoid muscle in the outstretched hand posture, producing clinically small jerks or loss of muscle tone when they stimulated the SMA with a single electric pulse stimulation of 1 Hz, like in the case of a part of primary sensorimotor cortex (Ikeda et al., 2000), but they did not observe motor evoked potentials or speech interruption. This may provide some clues that SMA can elicit contralateral, proximal weakness as seen in Patient 3, in addition to NMS from NMA. Because the number of patients was limited in the present study, it still remains to be established whether seizures from NMA also manifest focal ictal paresis in addition to NMS.

Rare incidence of NMS

In two patients (Patients 1 and 2), positive motor seizures subsequently occurred following NMS, and the two patients had a history of GTCS. Because these patients had frontal lobe epilepsy, it is very likely that ictal activity can spread easily to nonprimary and primary motor cortices, resulting in positive motor seizures, and subsequently GTCS.

NMS has rarely been described by video-EEG monitoring, although suspicious situations were documented in the literature before the development of video-EEG monitoring (Penfield & Jasper, 1954). NMS has never been precisely documented by invasive recording previously. It is probably because even though NMS occurred, the patient would not recognize it unless he allows himself to do voluntary movements during this period, as in the case of NMR with high-frequency stimulation. Furthermore, once the ictal activity responsible for NMS spreads into the adjacent nonprimary or primary motor cortices, the positive motor symptoms would obscure NMS. Although ictal activity that elicits positive motor seizures can spread into the NMA, the symptoms of NMS could be hidden by positive motor symptoms, or arrest of motion could not be tested because the consciousness is disturbed. The patients are not cooperative due to anxiety, or arrest of motion could be misinterpreted as a postictal exhausted condition.

In conclusion, when ictal activity arises from the NMA of either mesial or lateral frontal cortices, arrest of motion and vocalization occur, even though the patient is aware and comprehension is preserved, and thus it is called NMS. Clear weakness or decreased muscle tonus is not present, but very slight proximal weakness may be associated, which would reflect one of the functions of the NMA as well. Since focal ictal activity within the NMA could quickly spread to the adjacent primary or nonprimary motor cortices, elicited positive motor symptoms can obscure NMS. The symptoms of NMS may reflect ictal apraxia in an acute dynamic state of ictus, but this requires further investigation.

Acknowledgments

This study was supported by Grants-in-Aid for Scientific Research (C)(2) 18590935 for the Japan Society for the Promotion of Science (JSPS) and Research Grant for the Treatment of Intractable Epilepsy (19–1) from the Japan Ministry of Health, Labor and Welfare for A.I.

We confirm that we have read the Journal's position on issues involved in ethical publication and affirm that this report is consistent with those guidelines.

Disclosure: None of the authors has any conflict of interest to disclose.

References

Abou-Khalil B, Fakhoury T, Jennings M, Moots P, Warner J, Kessler RM. (1995) Inhibitory motor seizures: correlation with centroparietal structural and functional abnormalities. *Acta Neurol Scand* 91:103–108.

De Renzi E, Pieczuro A, Vignolo LA. (1966) Oral apraxia and aphasia. *Cortex* 2:50–73.

Engel J Jr. (2001) ILAE commission report. A proposed diagnostic schema for people with epileptic seizures and with epilepsy: report of the ILAE task force on classification and terminology. *Epilepsia* 42:796–803.

Engel J Jr. (2006) Report of the ILAE Classification Core Group. *Epilepsia* 47:1558–1568.

Fisher CM. (1978) Transient paralytic attacks of obscure nature: the question of nonconvulsive seizure paralysis. *Can J Neurol Sci* 5:267–273.

Gastaut H, Broughton R. (1972) *Epileptic seizures*. Charles C Thomas, Springfield.

Gowers WR. (1885) *Epilepsy and other chronic convulsive diseases*. Williams Woods, New York.

Guerrini R, Dravet C, Genton P, Bureau M, Roger J, Rubboli G, Tassinari CA. (1993) Epileptic negative myoclonus. *Neurology* 43:1078–1083.

Hamilton NG, Matthews T. (1979) Aphasia: the sole manifestation of focal status epilepticus. *Neurology* 29:745–748.

Hirasawa K, Muragaki Y, Yamane F, Hori T, Ikeda A, Ohara S. (2001) A case of mesial frontal glioma with ictal arrest of motions arising from the supplementary motor area. *J Jpn Epil Soc* 19:60. (abstract in Japanese).

Ikeda A, Lüders HO, Burgess RC, Shibasaki H. (1992) Movement-related potentials recorded from supplementary motor area and primary motor area : role of supplementary motor area in voluntary movements. *Brain* 115:1017–1043.

Ikeda A, Yazawa S, Kunieda T, Araki K, Aoki T, Hattori H, Taki W, Shibasaki H. (1997) Scalp-recorded focal, ictal DC shift in a patient with tonic seizure. *Epilepsia* 38:1350–1354.

Ikeda A, Taki W, Kunieda T, Terada K, Mikuni N, Nagamine T, Yazawa S, Ohara S, Hori T, Kaji R, Kimura J, Shibasaki H. (1999) Focal ictal DC shifts in human epilepsy as studied by subdural and scalp recording. *Brain* 122:827–838.

Ikeda A, Ohara S, Matsumoto R, Kunieda T, Nagamine T, Miyamoto S, Kohara N, Taki W, Hashimoto N, Shibasaki H. (2000) Role of primary sensorimotor cortices in generating inhibitory motor response in humans. *Brain* 123:1710–1721.

Ikeda A. (2003) Electrocorticography in motor control and movement disorders. In Hallett M (Ed.) *Handbook of Clinical Neurophysiology: Movement Disorders.* Elsevier, Amsterdam, pp. 31–44.

Ikeda A, Shibasaki H. (2003) Intracranial recording of Bereitschaftspotentials in patients with epilepsy. In Jahanshai J, Mallett M (Eds) *The Bereitschaftspotentials: Movement-related cortical potentials.* Kluwer Academic/Plenum, New York, pp. 45–59.

Imai H. (1996) Clinicophysiological features of akinesia. *Eur Neurol* 36(Suppl. 1):9–12.

Kertesz A, Hooper P. (1982) Praxis and language: the extent and variety of apraxia in aphasia. *Neuropsychologia* 20:275–286.

Kirshner HS, Hughes T, Fakhoury T, Abou-Khalil B. (1995) Aphasia secondary to partial status epilepticus of the basal temporal language area. *Neurology* 45:1616–1618.

Kunieda T, Ikeda A, Ohara S, Matsumoto R, Taki W, Hashimoto N, Baba K, Inoue Y, Mihara T, Yagi K, Shibasaki H. (2004) Role of the lateral non-primary motor area in humans as revealed by Bereitschaftspotential. *Exp Brain Res* 156:135–148.

Lakke PWF (Chairman of ad hoc Committee on Classification). (1981) Classification of extrapyramidal disorders. *J Neurol Sci* 51:311–327.

Lim SH, Dinner DS, Pillay PK, Lüders H, Morris HH, Klem G, Wyllie E, Awad IA. (1994) Functional anatomy of the human supplementary sensorimotor area: results of extraoperative electrical stimulation. *Electroencephalogr Clin Neurophysiol* 91:179–193.

Lüders H, Lesser RP, Dinner DS, Morris HH, Hahn JF, Friedman L, Skipper G, Wyllie W, Friedman D. (1987) Commentary: chronic intracranial recording and stimulation with subdural electrodes. In Engel J Jr (Ed.) *Surgical treatment of the epilepsies.* Raven Press, New York, pp. 297–321.

Lüders HO, Dinner DS, Morris HH, Wyllie E, Comair YG. (1995) Cortical electric stimulation in humans: the negative motor areas. In Fahn S, Hallett M, Lüders HO (Eds) *Negative motor phenomena. Advances in Neurology*, vol. 67. Lippincott-Raven, New York, pp. 115–1129.

Matelli M, Luppino G, Rizzolatti G. (1991) Architecture of superior and mesial area 6 and the adjacent cingulate cortex in the macaque monkey. *J Comp Neurol* 311:445–462.

Matsumoto R, Ikeda A, Hitomi T, Aoki T, Miki Y, Tomimoto H, Shimohama S, Shibasaki H. (2005) Ictal monoparesis associated with lesion in the primary somatosensory area. *Neurology* 65:1476–1478.

Meletti S, Rubboli G, Testoni S, Michelucci R, Cantalupo G, Stanzani-Maserati M, Calbucci F, Tassinari CA. (2003) Early ictal speech and motor inhibition in fronto-mesial epileptic seizures: a polygraphic study in one patient. *Clin Neurophysiol* 114:56–62.

Mikuni N, Ohara S, Ikeda A, Hayashi N, Nishida N, Taki J, Enatsu R, Matsumoto R, Shibasaki H, Hashimoto N. (2006) Evidence of a wide distribution of negative motor areas in the perirolandic cortex. *Clin Neurophysiol* 117:33–40.

Mikuni N, Okada T, Takin J, Matsumoto R, Nishida N, Enatsu R, Hanakawa T, Ikeda A, Miki Y, Urayama S, Fukuyama H, Hashimoto N. (2007) Fibers from the dorsal premotor cortex elicit motor evoked potential in a cortical dysplasia. *Neuroimage* 34:12–18.

Narabayashi H. (1980) Clinical analysis of akinesia. *J Neural Transm Suppl* 16:129–136.

Nii Y, Uematsu S, Lesser RP, Gordon B. (1996) Does the central sulcus divide motor and sensory functions? Cortical mapping of human hand areas as revealed by electrical stimulation through subdural grid electrodes. *Neurology* 46:360–367.

Noachtar S, Lüders HO. (1999) Focal akinetic seizures as documented by elecroencephalography and video recording. *Neurology* 53:427–429.

Noachtar S, Lüders HO. (2000) Akinetic seizures. In Lüders HO, Noachtar S (Eds) *The Epileptic Seizures: Pathophysiology and Semiology.* Churchill Livingstone, New York, pp. 489–500.

Penfield W, Rasmussen T. (1950) *The cerebral cortex of man. a clinical study of localization of function.* MacMillan Company, New York.

Penfield W, Jasper H. (1954) *Epilepsy and the functional anatomy of the human brain.* Little, Brown, Boston.

Rizzolatti G, Camarda R, Fogassi L, Gentilucci M, Luppino G, Matelli M. (1988) Functional organization of inferior area 6 in the macaque monkey. II. Area F5 and the control of distal movements. *Exp Brain Res* 71:491–507.

Rizzolatti G, Craighero L. (2004) The mirror-neuron system. *Annu Rev Neurosci* 2004:27.

Ropper AH, Brown RH. (2005) *Adams and Victor's Principles of Neurology.* 8th ed. McGraw-Hill, New York.

Rubboli G, Mai R, Meletti S, Francione S, Cardinale F, Tassi L, Lo Russo G, Stanzani-Maserati M, Cantalupo G, Tassinari CA. (2006) Negative myoclonus induced by cortical electrical stimulation in epileptic patients. *Brain* 129:65–81.

Salanova V, Andermann F, Rasmussen T, Olivier A, Quesney LF. (1995) Parietal lobe epilepsy. Clinical manifestations and outcome in 82 patients treated surgically between 1929 and 1988. *Brain* 118:607–627.

So NK. (1995) Atonic phenomena and partial seizures, a reappraisal. In Fahn S, Hallett M, Lüders HO (Eds) *Negative motor phenomena. Advances in Neurology*, vol.67. Lippincott-Raven, New York, pp. 29–39.

Villani F, D'Amico D, Pincherle A, Tullo V, Chiapparini L, Bussone G. (2006) Prolonged focal negative motor seizures: a video-EEG study. *Epilepsia* 47:1949–1952.

Watson RT, Gnzales Rothi LJ, Heilman KM. (1992) Apraxia: a disorder of motor programming. In Joseph AB, Young RR (Eds) *Movement disorders in Neurology and Neuropsychiatry*, Chapter 87, Blackwell, Boston, pp. 681–695.

Yazawa S, Ikeda A, Kunieda T, Ohara S, Mima T, Nagamine T, Taki W, Hori T, Shibasaki H. (2000) Human pre-supplementary motor area is active before voluntary movement: subdural recording of Bereitschaftspotentials from mesial frontal cortex. *Exp Brain Res* 131:165–177.

Cortical microinfarcts in Alzheimer's disease and subcortical vascular dementia

Yoko Okamoto[a], Masafumi Ihara[a], Youshi Fujita[a], Hidefumi Ito[a], Ryosuke Takahashi[a] and Hidekazu Tomimoto[b]

Cortical microinfarcts are reported in Alzheimer's disease, but not in subcortical vascular dementia; the disease specificity of cortical microinfarcts therefore remains unclear. The distribution of cortical microinfarcts in Alzheimer's disease ($n=8$) and subcortical vascular dementia ($n=6$) was analyzed. Cortical microinfarcts were frequently detected in Alzheimer's disease, whereas they were rarely observed in subcortical vascular dementia. In Alzheimer's disease, cortical microinfarcts were present predominantly in the occipital lobe, the area of predilection for amyloid angiopathy, and also in the vascular borderzone. Cortical microinfarcts were invariably located very close to amyloid β-deposited vessels with intercellular adhesion molecule-1 expression. These results indicate that cortical microinfarcts are caused by the pathomechanism related to Alzheimer's disease, most likely to amyloid angiopathy. *NeuroReport* 20:990–996

NeuroReport 2009, 20:990–996

Keywords: Alzheimer's disease, amyloid angiopathy, cortical microinfarct, subcortical vascular dementia

[a]Department of Neurology, Graduate School of Medicine, Kyoto University, Kyoto and [b]Department of Neurology, Graduate School of Medicine, Mie University, Mie, Japan

Correspondence to Dr Yoko Okamoto, Department of Neurology, Graduate School of Medicine, Kyoto University, 54 Kawaharacho, Shogoin, Sakyo-ku, Kyoto 606-8507, Japan
Tel/fax: +81 75 751 3766; e-mail: yoko416@kuhp.kyoto-u.ac.jp

Received 14 March 2009 accepted 17 April 2009

Introduction

Recently, an increasing body of evidence has indicated that vascular risk factors, such as hypertension and diabetes mellitus have a pivotal role in the pathogenesis of Alzheimer's disease [1]. Accordingly, the Nun study has shown that the risk of dementia increases more than 20 times in Alzheimer's disease, if the patients have foci of cerebral infarctions [2]. Cortical microinfarcts were predominantly observed in the vascular borderzone of Alzheimer's disease brains [3], and were found to be a strong determinant for dementia, in a manner comparable with the neuropathological hallmarks that determine Alzheimer's disease [4–6].

The pathoetiology and disease specificity of cortical microinfarcts remain elusive. It is unclear whether cortical microinfarcts are present exclusively in Alzheimer's disease brains, or are associated with hypertensive small-vessel disease. In this study, we compared the distribution of cortical microinfarcts in Alzheimer's disease and subcortical vascular dementia, focusing especially on their spatial correlation with amyloid angiopathy.

Materials and methods

Human tissue

Two hundred and seventy autopsied brains were obtained from the Kyoto University Hospital and its affiliated hospitals from 1988 to 2007 through a process approved by an institutional research committee. Among the 270 brains, there included 13 Alzheimer's disease brains and six subcortical vascular dementia brains. We excluded five Alzheimer's disease brains because of concomitant macroscopic cerebral infarctions. We examined the remaining eight Alzheimer's disease brains (mean ± SEM: 79 ± 4 years old) and six subcortical vascular dementia brains (mean ± SEM: 77 ± 5 years old). These Alzheimer's disease and subcortical vascular dementia patients met the diagnostic criteria for dementia (*Diagnostic and Statistical Manual of Mental Disorders*, fourth edition) [7]. The diagnosis of Alzheimer's disease was based on the Consortium to Establish a Registry for Alzheimer's Disease diagnostic neuropathologic criteria [8], and the Braak and Braak neuropathological staging of Alzheimer-related changes [9].

The diagnosis of subcortical vascular dementia was made clinicopathologically to meet the criteria of: (i) the presence of bilateral diffuse subcortical lesions, (ii) lacunar infarctions in the perforator territory, (iii) arteriolosclerosis, such as fibrohyalinosis and fibrinoid necrosis, and (iv) the absence of cortical infarctions, and the clinical criteria outlined by Bennett *et al.* [10]. Cases with significant pathological hallmarks of Alzheimer's disease (senile plaque Braak stage ≥ B, neurofibrillary tangle Braak stage ≥ II [9]) were excluded.

Immunohistochemical staining

Tissue blocks obtained from the frontal, temporal, parietal, and occipital lobes were embedded in paraffin. Histological assessment was carried out with hematoxylin and eosin (H&E), Klüver–Barrera, and modified Bielschowsky staining. The rest of the blocks were used for immunohistochemistry as described earlier [11]. The

0959-4965 © 2009 Wolters Kluwer Health | Lippincott Williams & Wilkins

DOI: 10.1097/WNR.0b013e32832d2e6a

primary antibodies consisted of: rabbit anti-glial fibrillary acidic protein (GFAP) (diluted 1:200; Dako, Glostrup, Denmark), mouse anti-human cluster of differentiation 68 (CD68) (1:100; Dako), mouse anti-amyloid β-protein (1:100; Novocastra, Newcastle, UK), and mouse anti-intercellular adhesion molecule-1 (ICAM-1) (1:100; Santa Cruz Biotechnology, Santa Cruz, California, USA). For IgG, horseradish peroxidase-labeled anti-human IgG (1:50; Dako), and for actin, rhodamin-labeled phalloidin (1:200; Invitrogen Corporation, Carlsbad, California, USA) were used.

Image analysis

Images of the histological slides were captured with a digital camera (CAMEDIA C-7070; Olympus, Tokyo, Japan) and scanned (Canon, CanoScan N1220U; Canon Inc., Tokyo, Japan). In each slide, cortical areas were outlined and the corresponding numbers of pixels were counted using the ImageJ software package (National Institute of Health; Bethesda, Maryland, USA).

Definition and count of cortical microinfarcts

Cortical microinfarcts had not been defined earlier, and were therefore determined according to the following criteria: a cortical lesion that was not noticeable until examined microscopically and accompanied by a group of astrocyte or microglia/macrophage proliferation. Histological changes likely to be expanded Virchow–Robin spaces, microabscesses, or cortical laminar necrosis were excluded.

After measuring the number of microinfarcts and the cortical area in each specimen, we calculated the number of cortical microinfarcts (per cm^2) infiltrated by numerous GFAP-positive astrocytes or CD68-positive microglia/macrophages.

The cerebral cortex was divided into five regions according to the arterial supply of anterior, middle, and posterior cerebral arteries, and their two borderzones (anterior-middle and middle-posterior), based on the text atlas [12]. The borderzone was defined as the area within 3 cm apart from the proposed borderline [12], and the number of microinfarcts was calculated similarly as stated above. The distribution of microinfarcts was further studied in terms of their topographic relationships to the cortical layers and the cerebral convolutions. Briefly, microinfarcts were classified into those distributed in layers 1–3 or 4–6, or alternatively, into those located in the crown part, the sulcal part, or the depth of the sulcal part.

The topographical relationship between Aβ-positive vessels and microinfarcts was also assessed. Microinfarcts were judged to adjoin Aβ-deposited vessels, if they were localized within 1 mm of these vessels. Senile plaque load was assessed with modified Bielschowsky staining in the region containing each microinfarct. The severity of senile plaque load was divided into four groups: those with none, sparse, moderate, and frequent in accordance with the Consortium to Establish a Registry for Alzheimer's Disease criteria [8].

Statistical analysis

Data were statistically analyzed using one-way analysis of variance, followed by Bonferroni's post-hoc test (Statview version 5.0, SAS Institute, Cary, North Carolina, USA).

Results

All microinfarcts detected in H&E stains were invariably accompanied by GFAP-positive astroglia. The mean diameter of the microinfarcts was approximately 200 μm (range 100–500). Cortical microinfarcts were found in all

Fig. 1

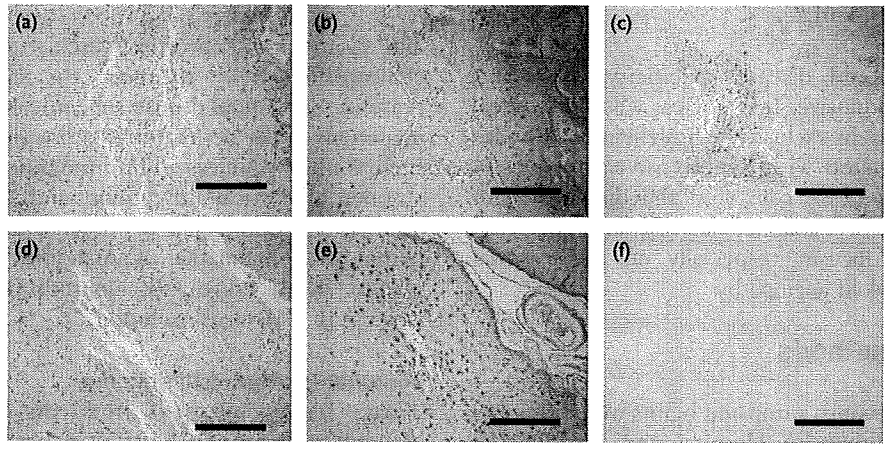

Photomicrographs of cortical microinfarcts with (a–c) and without microglial activation (d–f). The upper panels (a–c) and lower panels (d–f) are adjacent sections. Hematoxylin and eosin staining (a, d), immunohistochemistry for glial fibrillary acidic protein (GFAP; b, e), and cluster of differentiation 68 (CD68; c, f). Bars indicate 300 μm.

eight Alzheimer's disease brains and one of the six subcortical vascular dementia brains, and were classified into two groups: microinfarcts with or without infiltration of CD68-positive microglia/macrophages (Fig. 1). The lesions that had been infiltrated both by astroglia and microglia/macrophages were considered to be relatively recent infarcts. The lesions with astrogliosis, but without CD68-positive microglia/macrophages, were considered to be older. This is because both astroglia and microglia/macrophages are activated in the acute stage of cerebral infarction, but macrophages regress within several months.

In H&E stains, lesions accompanied by erythrocytes or hemosiderin depositions were excluded. Furthermore, Perls–Stieda staining was added to search for iron deposits and IgG immunohistochemistry for serum protein extravasation, so that microhemorrhagic lesions could be ruled out. Only a minority (3%) of cortical microlesions were accompanied by iron deposits or IgG-positive astroglia, indicating that most microlesions are not caused by hemorrhagic mechanisms (compare Fig. 2a and c, and Fig. 2b and d).

Fig. 2

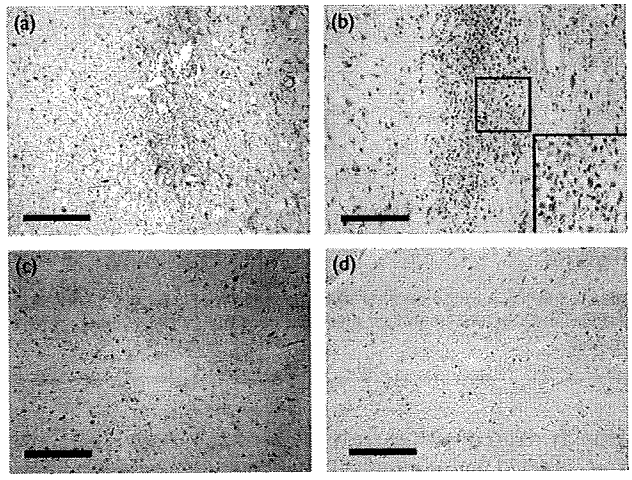

Photomicrographs of cortical microinfarcts (CMIs) with immunohistochemical staining for IgG (a, c) and Perls–Stieda staining to detect iron depositions (b, d). Note IgG-positive astroglia (a) or iron deposits (b, inset). (c) and (d) show CMIs without IgG-positive glia or iron deposits, respectively. Bars in (a) indicate 250 μm, and in (b–d) 200 μm.

The numerical densities of cortical microinfarcts with GFAP-positive astroglia in Alzheimer's disease were 0.45, 0.14, 0.43, and 1.08 (per cm^2) in the frontal, temporal, parietal, and occipital lobes, respectively. The densities of cortical microinfarcts with CD68-positive microglia/macrophages were 0.11, 0.04, 0.00, and 0.44, respectively, in each lobe (Table 1 and Fig. 3a). In contrast, in subcortical vascular dementia, the numerical densities of cortical microinfarcts with GFAP-positive astroglia were 0.058, 0.015, 0, and 0, respectively, in each lobe (per cm^2) (Table 1). Thus, cortical microinfarcts were frequent in Alzheimer's disease, but were rarely found in subcortical vascular dementia.

In Alzheimer's disease, there was a marginally significant increase of microinfarcts with GFAP-positive astroglia in the occipital lobe compared with the temporal lobe ($P = 0.0511$), whereas there was only an increased tendency compared with the other lobes (occipital vs. frontal, $P = 0.1709$; frontal vs. parietal, $P = 0.9775$; frontal vs. temporal, $P = 0.5118$). In terms of the arterial supply, the numerical densities of cortical microinfarcts with GFAP-positive astroglia were 0.40, 0.19, 0.28, 0.66, and 1.47 (per cm^2) in Alzheimer's disease in the anterior, middle, and posterior cerebral arteries, anterior-middle cerebral arterial boderzone, and middle-posterior cerebral arterial borderzone, respectively (Table 1 and Fig. 3b). Most of the microinfarcts were distributed in the superficial borderzones. In terms of cortical layers, the number of microinfarcts with GFAP-positive astroglia was significantly different between the superficial and the deep

Table 1 The distribution of microinfarcts in different cortical regions

	Layer		Convolution[a]			AA	Lobe (per 1 cm^2)[b]				Vascular territory (per 1 cm^2)[c]					SP[d]			
Number of cortical microinfarcts	1–3	4–6	C	S	D	(+)	F	T	P	O	A	A/M	M	M/P	P	N	S	M	F
AD (n=8)																			
HE	40	9	25	1	23	26/49	0.28	0.08	0.20	0.44	0.16	0.37	0.07	0.82	0.00	0	13	19	17
GFAP	73	19	42	8	42	46/92	0.45	0.14	0.43	1.08	0.40	0.66	0.19	1.47	0.28	0	25	42	25
CD68	15	5	10	0	10	16/20	0.11	0.04	0.00	0.44	0.07	0.21	0.02	0.68	0.00	0	9	11	0
SVD (n=6)																			
HE	4	0	1	1	2	0/4 (0%)	0.043	0.015	0	0	0	0.029	0	0	0.028	4	0	0	0
GFAP	5	0	2	1	2	0/5 (0%)	0.058	0.015	0	0	0	0.048	0	0	0.028	5	0	0	0
CD68	4	0	1	1	2	0/4(0%)	0.043	0.015	0	0	0	0.029	0	0	0.028	4	0	0	0

AA, amyloid angiopathy; +, the rate of AA-positive cortical microinfarcts; AD, Alzheimer's disease; HE, hematoxylin and eosin; GFAP, glial fibrillary acidic protein; CD68, cluster of differentiation 68; SVD, subcortical vascular dementia.
[a]C, crown part; D, depth; S, sulcal part.
[b]F, frontal; O, occipital; P, parietal; T, temporal.
[c]A, A/M, M, M/P, P denotes anterior, middle, and posterior cerebral arteries, and their borderzones, respectively.
[d]F, frequent; M, moderate; N, none; S, sparse; SP, senile plaque.

Fig. 3

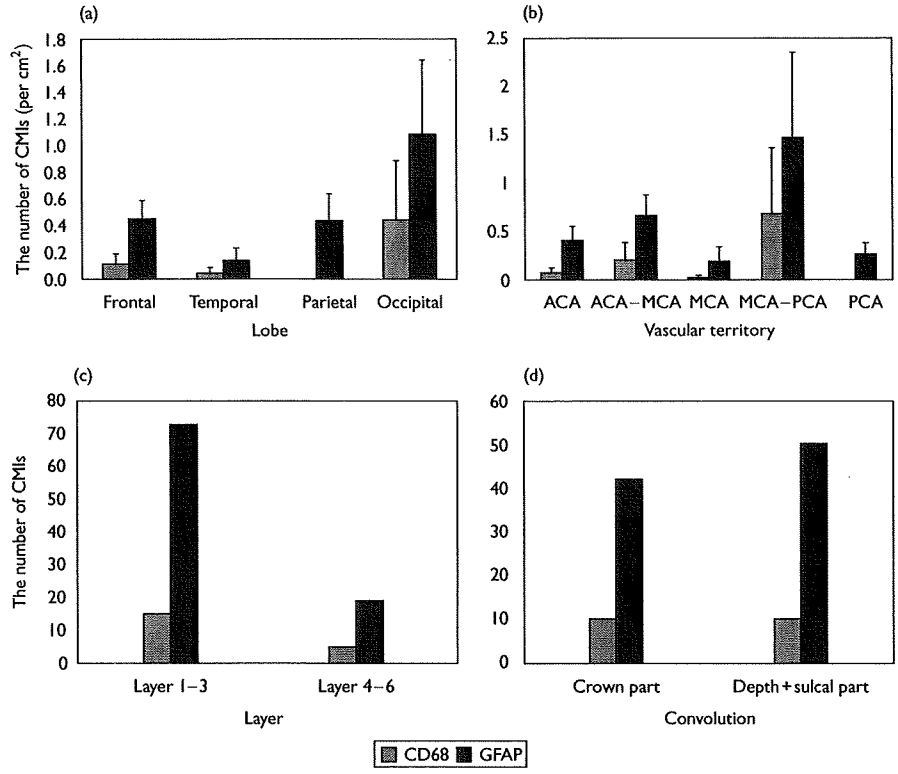

The density of cortical microinfarcts (CMIs/cm^2) in each lobe (a) and vascular territories (b), and the number of CMIs in cortical layers (c) and inside the cerebral convolutions (d). ACA, MCA, PCA, A/M, M/P denote anterior, middle, and posterior cerebral arteries, and their borderzones, respectively. CD68, cluster of differentiation 68; GFAP, glial fibrillary acidic protein.

layers of the Alzheimer's disease brains (73 vs. 19, respectively, $P = 0.0080$ by one-way analysis of variance) (Table 1 and Fig. 3c). However, no trends were found in terms of spatial distribution within the cerebral convolution (Table 1 and Fig. 3d).

Aβ-immunoreactive vessels were observed in six cases of the eight Alzheimer's disease brains, but not in six subcortical vascular dementia brains. Interestingly, Aβ deposition was predominantly in the vessels apposed to microinfarcts (Fig. 4). Such vessels were tortuous or double-barrel in shape. Half of the cortical microinfarcts with GFAP-positive astroglia (46 out of the 92) were localized less than 1 mm apart from Aβ-positive vessels. ICAM-1 was preferentially expressed in the endothelial cells and vessel walls surrounding microinfarcts (Fig. 5a and b). Double labeling for ICAM-1 and actin showed that the vessels around microinfarcts commonly express ICAM-1 (Fig. 5c–e). The number of microinfarcts was not associated with senile plaque burden (Table 2).

Discussion

Sporadic cerebral amyloid angiopathy (CAA) is a state in which Aβ deposits in the cerebral vessels, and has been strongly related with the presence of dementia [13]. Thal *et al.* [14,15] have reported two types of sporadic CAA: capillary CAA and classical CAA. In capillary CAA, Aβ deposits are present within capillaries; whereas in classical CAA, Aβ initially deposits at the outer basement membrane of the leptomeningeal and cortical arteries, and then within their smooth muscle layer [14,15]. As both the capillary and classical CAA pathologies were present in most of the brains with Alzheimer's disease, further investigation is required to know which of the two pathologies underlies cortical microinfarcts.

CAA is dormant during lifetime, whereas it leads to major cerebral hemorrhage (approximately 5–20%) or infarct in a subset of elderly patients [16]. As a facilitating factor, the ApoE ε2 and ε4 alleles are related to a higher risk for CAA or CAA-associated hemorrhage [14–16]. In this study, the ApoE genotype was not assessed; therefore, it remains unknown whether there is a relationship between ApoE genotype and cortical microinfarcts in Alzheimer's disease.

The occipital lobe is most commonly and severely affected in CAA [14–16]. In this study, GFAP-positive

Fig. 4

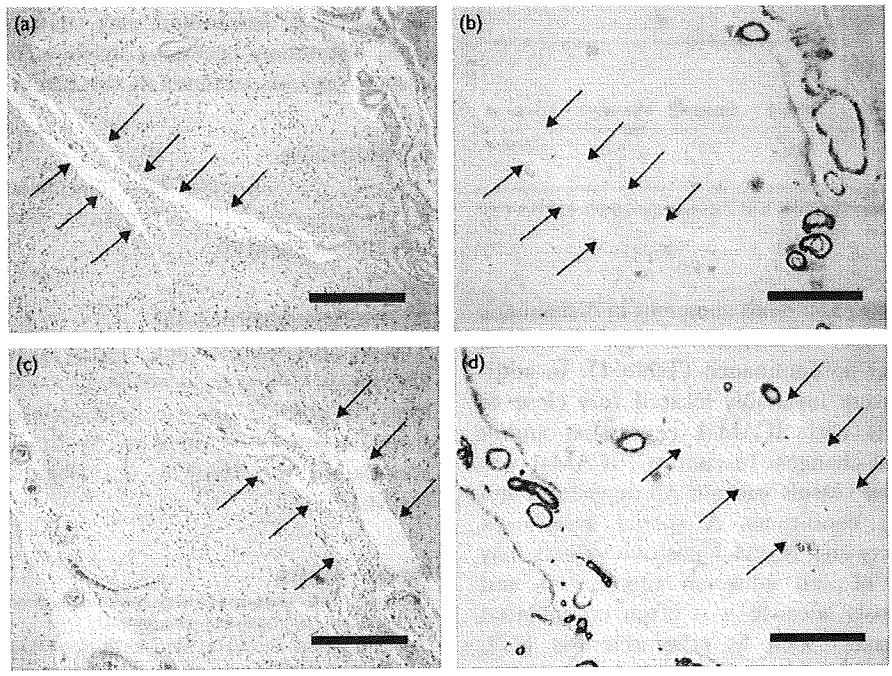

Photomicrographs of cortical microinfarcts with hematoxylin and eosin staining (a, c) and immunohistochemistry for Aβ (b, d). The upper panels (a, b) and lower panels (c, d) are adjacent sections. Arrows indicate microinfarcts. Bars in (a–d) indicate 250 μm.

Fig. 5

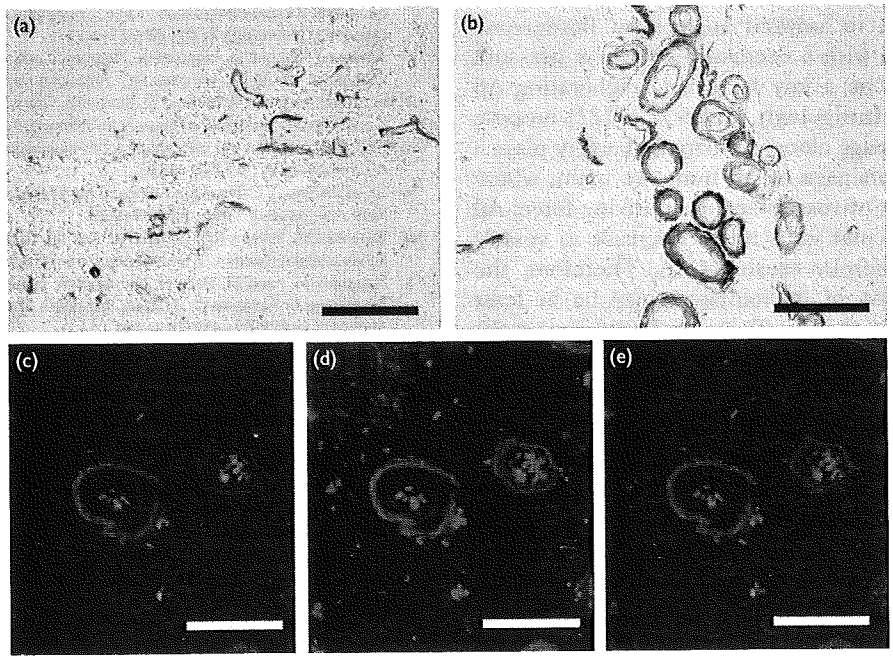

Photomicrographs of immunohistochemistry for intercellular adhesion molecule-1 (ICAM-1) (a–c), actin (d), and double labeling for ICAM-1 and actin (e). Bars in (a), (c–e) indicate 100 μm, and in (b) 200 μm.

Table 2 The number of GFAP-positive or CD68-positive cortical microinfarcts and their associations with senile plaque burden

		SP			
Cortical microinfarcts	Total number of cortical microinfarcts	None	Sparse	Moderate	Frequent
GFAP-positive	92	0	25	42	25
CD68-positive	20	0	9	11	0

CD68, cluster of differentiation 68; GFAP, glial fibrillary acidic protein; SP, senile plaque.

cortical microinfarcts were far more numerous in Alzheimer's disease compared with subcortical vascular dementia, and showed occipital predominance (Table 1). In addition, microinfarcts were invariably located very close to Aβ-deposited vessels with ICAM-1 expression and/or severe morphological changes. In contrast, ICAM-1 was rarely detected in the vessels without Aβ deposition and those in quiescent conditions. A spatial association between microinfarcts and ICAM-1 positive vessels may indicate activation of cell adhesion mechanism and subsequent thrombosis because it is often upregulated in inflammatory states, such as atherosclerosis [17]. In correspondence with these findings, occipital predominance has also been revealed in the distribution of microbleeds, which are also attributed to CAA [18].

Microinfarcts were distributed not only in the occipital lobe, but also in the superficial borderzone, in accordance with the earlier study [3]. Predilection of microinfarcts in the borderzone territory suggests that hypoperfusion in these areas contributes to the pathogenesis of microinfarcts in addition to amyloid angiopathy. Borderzone territory is irrigated with a decreased perfusion pressure [19] and this may be a key factor in ameliorating Aβ deposition [20,21]. Intriguingly, Weller *et al.* [22] propose that lymphatic drainage along capillary and artery plays a significant role in drainage of Aβ from the brain, where pulsatile movement of vessels acts as a driving force. Aβ clearance along vascular walls might decrease as vessels stiffen with age, thereby causing CAA. Therefore, the observed predilection of microinfarcts may be at least partially explained by the insufficient pulsatile movement and augmented Aβ deposition in the borderzone area.

In an earlier study, this group has reported cortical microvascular changes in Alzheimer's disease and their absence in subcortical vascular dementia [11]. The capillary densities in Alzheimer's disease were significantly decreased with various morphological changes, such as tearing or narrowing of the cortical microvessels. Furthermore, Stopa *et al.* [23] have reported that smooth muscle actin is decreased in the arterioles even from the early stages of Alzheimer's disease. In contrast to the medullary arteries, which consistently show arteriosclerotic changes in the white matter, small vessel changes were rarely found in the cerebral cortices of subcortical vascular dementia. Different patterns of small vessel changes in topographical distribution may consequently explain the clear distinction between Alzheimer's disease and subcortical vascular dementia in terms of cortical microinfarcts.

Conclusion

Cortical microinfarcts may be caused by the pathomechanism related to Alzheimer's disease, most likely to amyloid angiopathy.

Acknowledgements

The authors express their cordial gratitude to Dr Ahmad Khundakar for critical reading of the manuscript and Miss Nakabayashi for excellent technical assistance. This study is supported, in part, by the Mochida Memorial Foundation for Medical and Pharmaceutical Research (to M.I.).

References

1 Kalaria RN. Similarities between Alzheimer's disease and vascular dementia. *J Neurol Sci* 2002; **203–204**:29–34.
2 Snowdon DA, Greiner LH, Mortimer JA, Riley KP, Greiner PA, Markesbery WR. Brain infarction and the clinical expression of Alzheimer disease. The Nun Study. *JAMA* 1997; **277**:813–817.
3 Suter OC, Sunthorn T, Kraftsik R, Straubel J, Darekar P, Khalili K, *et al.* Cerebral hypoperfusion generates cortical watershed microinfarcts in Alzheimer disease. *Stroke* 2002; **33**:1986–1992.
4 White L, Petrovitch H, Hardman J, Nelson J, Davis DG, Ross GW, *et al.* Cerebrovascular pathology and dementia in autopsied Honolulu-Asia Aging Study participants. *Ann NY Acad Sci* 2002; **977**:9–23.
5 Kövari E, Gold G, Herrmann FR, Canuto A, Hof PR, Michel JP, *et al.* Cortical microinfarcts and demyelination significantly affect cognition in brain aging. *Stroke* 2004; **35**:410–414.
6 Kövari E, Gold G, Herrmann FR, Canuto A, Hof PR, Bouras C, *et al.* Cortical microinfarcts and demyelination affect cognition in cases at high risk for dementia. *Neurology* 2007; **68**:927–931.
7 American Psychiatric Association. *Diagnostic and Statistical Manual of Mental Disorders*. 4th ed. Washington DC: American Psychiatric Association; 1994.
8 Mirra SS, Heyman A, McKeel D, Sumi SM, Crain BJ, Brownlee LM, *et al.* The Consortium to Establish a Registry for Alzheimer's Disease (CERAD). Part II. Standardization of the neuropathologic assessment of Alzheimer's disease. *Neurology* 1991; **41**:479–486.
9 Braak H, Braak E. Neuropathological staging of Alzheimer-related changes. *Acta Neuropathol* 1991; **82**:239–259.
10 Bennett DA, Wilson RS, Gilley DW, Fox JH. Clinical diagnosis of Binswanger's disease. *J Neurol Neurosurg Psychiatry* 1990; **53**:961–965.
11 Kitaguchi H, Ihara M, Saiki H, Takahashi R, Tomimoto H. Capillary beds are decreased in Alzheimer's disease, but not in Binswanger's disease. *Neurosci Lett* 2007; **417**:128–131.
12 Kretschmann HJ, Weinrich W. *Neuroanatomy and cranial computed tomography*. New York, USA: Thieme-Stratton Corp.; 1986.
13 Neuropathology Group of the Medical Research Council Cognitive Function and Aging Study. Pathological correlates of late-onset dementia in a multicentre, community-based population in England and Wales. *Lancet* 2001; **357**:169–175.
14 Thal DR, Griffin W ST, de Vos R AI, Ghebremedhin E. Cerebral amyloid angiopathy and its relationship to Alzheimer's disease. *Acta Neuropathol* 2008; **115**:599–609.
15 Thal DR, Ghebremedhin E, Rüb U, Yamaguchi H, Tredici KD, Braak H. Two types of sporadic cerebral amyloid angiopathy. *J Neuropathol Exp Neurol* 2002; **61**:282–293.
16 Attems J. Sporadic cerebral amyloid angiopathy: pathology, clinical implications, and possible pathomechanisms. *Acta Neuropathol* 2005; **110**:345–359.
17 Braun M, Pietsch P, Schrör K, Braumann G, Felix SB. Cellular adhesion molecules on vascular smooth muscle cells. *Cardiovascular Research* 1999; **41**:395–401.

18 Pettersen JA, Sathiyamoorthy G, Gao FQ, Szilagyi G, Nadkarni NK, St George-Hyslop P, *et al.* Microbleed topography, leukoaraiosis, and cognition in probable Alzheimer disease from the Sunnybrook Dementia Study. *Arch Neurol* 2008; **65**:790–795.
19 Torvik A. The pathogenesis of watershed infarcts in the brain. *Stroke* 1984; **15**:221–223.
20 Ihara M, Kalaria RN. Amyloid-β and synaptic activity in mice and men. *Neuroreport* 2007; **18**:1205–1206.
21 Román GC, Kalaria RN. Vascular determinants of cholinergic deficits in Alzheimer disease and vascular dementia. *Neurobiol Aging* 2006; **27**:1769–1785.
22 Weller RO, Djuanda E, Yow HY, Carare RO. Lymphatic drainage of the brain and the pathophysiology of neurological disease. *Acta Neuropathol* 2009; **117**:1–14.
23 Stopa EG, Butala P, Salloway S, Johanson CE, Gonzalez L, Tavares R, *et al.* Cerebral cortical arteriolar angiopathy, vascular beta-amyloid, smooth muscle actin, Braak stage, and APOE genotype. *Stroke* 2008; **39**: 814–821.

Int. J. Cancer: **125,** 2029–2035 (2009)

Attenuation of proteolysis-mediated cyclin E regulation by alternatively spliced *Parkin* in human colorectal cancers

Kyoko Ikeuchi[1], Hiroyuki Marusawa[1]*, Mikio Fujiwara[1], Yuko Matsumoto[1], Yoko Endo[1], Tomohiro Watanabe[1], Akio Iwai[1], Yoshiharu Sakai[2], Ryosuke Takahashi[3] and Tsutomu Chiba[1]

[1]*Department of Gastroenterology and Hepatology, Graduate School of Medicine, Kyoto University, Kyoto, Japan*
[2]*Department of Gastrointestinal Surgery, Graduate School of Medicine, Kyoto University, Kyoto, Japan*
[3]*Department of Neurology, Graduate School of Medicine, Kyoto University, Kyoto, Japan*

Parkin has a critical role in the ubiquitin-proteasome system as an E3-ligase targeting several substrates. Our recent finding that *Parkin*-deficient mice are susceptible to tumorigenesis provided evidence that *Parkin* is a tumor suppressor gene. Dysfunction of the *Parkin* gene is frequently observed in various human cancers, but the mechanism underlying the cell cycle disruption induced by Parkin dysfunction that leads to carcinogenesis is not known. Here, we demonstrated that Parkin expression in colonic epithelial cells is regulated in a cell cycle-associated manner. Epidermal growth factor (EGF) stimulation upregulated *Parkin* gene expression in human colon cells. Inhibition of the phosphoinositide 3-kinase [PI(3)K]-Akt-dependent pathways suppressed growth factor-induced Parkin expression. The expression of alternatively spliced *Parkin* isoforms with various deletions spanning exons 3–6 was detected in 18 of 43 (42%) human colorectal cancer tissues. Wild-type *Parkin* induced the degradation of cyclin E protein, but the alternatively spliced *Parkin* identified in colon cancers showed defective proteolysis of cyclin E. These findings indicate that Parkin expression is induced by growth factor stimulation and is involved in the cell cycle regulation of colon cells. Tumor-specific expression of alternatively spliced *Parkin* isoforms might contribute to enhanced cell proliferation through the attenuation of proteolysis-mediated cyclin E regulation in human colorectal cancers.

Key words: Parkin; colorectal cancer; cyclin E; cell cycle; EGF

Parkin functions in the ubiquitin-proteasome system as an E3 ligase, facilitating the ubiquitination of target proteins.[1–3] Parkin is developmentally regulated with induced expression during cell differentiation, and little to no expression in immature cells.[4] Several putative candidate substrates of Parkin-mediated proteolysis have been identified, including α-synphilin, α-synuclein interacting protein, synphilin-1 and Pael-R.[5,6] Recently, it was revealed that deficiency of *Parkin* potentiates the accumulation of cyclin E protein in cultured postmitotic neurons exposed to the glutamatergic excitotoxin kainate, suggesting that the cell cycle regulator, cyclin E, is a putative substrate of the Parkin ubiquitin ligase complex in neurons.[7] Since *Parkin* was first identified as a gene implicated in autosomal recessive juvenile Parkinsonism, one form of familial Parkinson disease,[8] attention has been focused on unveiling the role of Parkin in neurons. The expression and regulation of Parkin in epithelial cells as well as the role of Parkin in cell cycle regulation, however, has not been clarified.

A loss of heterozygosity within chromosomal region 6q25-q27 containing the *Parkin* gene is frequently observed in various human tumors, including ovarian,[9–11] breast,[12] renal[13] and lung cancers.[14,15] In addition, the *Parkin* gene is frequently deleted in breast, ovarian and liver cancers.[16–18] We recently demonstrated that *Parkin*-deficient mice lacking exon 3 of the *Parkin* gene developed hepatocellular carcinoma, whereas *Parkin*$^{-/-}$ mice were neurologically normal with no obvious neuropathologic changes.[19] Further, the loss of *Parkin* expression contributes to the overproliferation of hepatocytes leading to hepatomegaly, suggesting a critical role for Parkin in the regulation of hepatocyte proliferation.[19] These observations suggest that *Parkin* has a role as a tumor suppressor and may be involved in cell cycle regulation in epithelial cells.

Deregulation of the cell cycle, specifically the G1 and S phases, is a hallmark of human cancers, and *cyclin E* amplification and overexpression are observed in various human cancers.[20] One thing to be noted is that cyclin E protein is accumulated in the tumor cells in a considerable proportion of colorectal cancers.[21] On the basis of these observations, in the present study, we evaluated the regulation of *Parkin* gene expression in association with cell cycle regulation in colonic epithelial cells.

Material and methods

Cell culture and transfection

The human colorectal cancer cell lines, HT29, SW48 and kidney-derived 293T cell lines were maintained in Dulbecco's modified Eagle's medium (Gibco-BRL, Tokyo, Japan) containing 10% fetal bovine serum. The human colorectal cancer-derived LoVo cells were cultured in Ham's F12 (MP Biomedicals, Solon, OH) containing 10% fetal bovine serum. Plasmid transfection was performed using Lipofectamine 2000 (Invitrogen, Carlsbad, CA) according to the manufacturer's protocol.

Plasmids and reagents

The expression plasmids pcDNA3-*Parkin* and pcDNA3-Δ-*Parkin* were described previously.[2] The expression plasmids pcDNA3-*Akt* and pcDNA3-*Akt (AA)*, encoding the wild-type and dominant negative mutants of human *Akt* with substitution of Thr308 and Ser473 by Ala,[22] respectively, were made by inserting the PCR-amplified cDNA fragment of human *Akt* sequences. Recombinant human epidermal growth factor (EGF) and hepatocyte growth factor (HGF) were obtained from Peprotech EC (London, UK). Mitogen-activated protein kinase kinase (MEK) inhibitor PD98059 and phosphoinositide 3-kinase [PI(3)k] inhibitor wortmannin were purchased from Promega (Madison, WI) and Sigma Chemical (St. Louis, MO), respectively. MG132 was obtained from Peptide Institute (Osaka, Japan). Small interference RNA (siRNA) duplexes composed of 21-nucleotide sense and antisense strand used for targeting *Parkin* were obtained from Invitrogen.

Additional Supporting Information may be found in the online version of this article.

Abbreviations: cdk, cyclin-dependent kinases; EGF, epidermal growth factor; HGF, hepatocyte growth factor; IBR, in-between Ring; MEK, mitogen-activated protein kinase kinase; MAPK, mitogen-activated protein kinase; PI(3)K, phosphoinositide 3-kinase; RING, really interesting new gene; RT-PCR, reverse transcription polymerase chain reaction; 18s rRNA, 18s ribosomal RNA; siRNA, small interference RNA; UBL, ubiquitin-like; UPD, unique Parkin domain.

Grant sponsor: Grants-in-aid for Scientific Research (The Ministry of Education, Culture, Sports, Science, and Technology of Japan); Grant numbers: 8209027, 20012029, 20590774.

***Correspondence to:** Department of Gastroenterology and Hepatology, Graduate School of Medicine, Kyoto University, 54 Kawara-cho, Shogoin, Sakyo-ku, Kyoto 606-8507, Japan. Fax: +81-75-751-4303.
E-mail: maru@kuhp.kyoto-u.ac.jp

Received 16 October 2008; Accepted after revision 21 April 2009
DOI 10.1002/ijc.24565
Published online 11 May 2009 in Wiley InterScience (www.interscience.wiley.com).

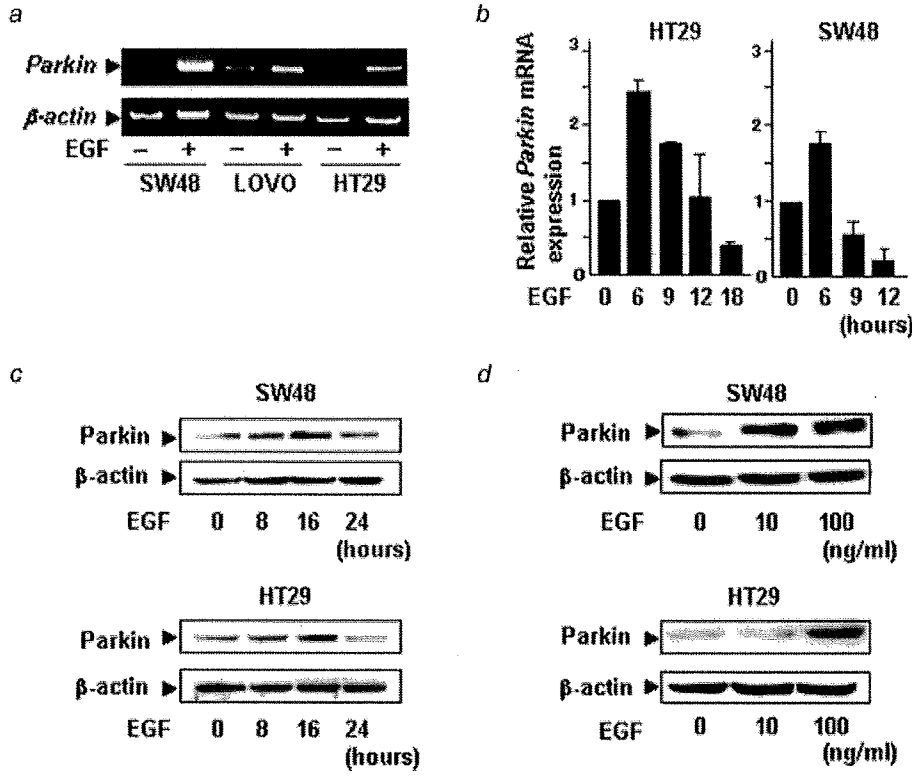

FIGURE 1 – Parkin expression is induced in response to EGF stimulation in colon cells. (*a*) SW48, LoVo and HT29 cells were treated with human recombinant EGF (100 ng/ml) and total RNA was isolated 6 hr after EGF treatment. RT-PCR was performed using 1 μg of each RNA sample as a template and oligonucleotide primers for human *Parkin* (upper panel) and *β-actin* (lower panel). (*b*) Time-course changes of *Parkin* mRNA expression after EGF stimulation. SW48 or HT29 cells were subjected to total RNA isolation immediately before and 6, 9, 12 and 18 hr after treatment with EGF. Real-time RT-PCR was performed using FAM-labeled probes specific for human *Parkin*. (*c*) SW48 or HT29 cells were treated with EGF (100 ng/ml) for 0, 8, 16 and 24 hr, followed by immunoblotting using anti-Parkin antibody (upper panel) or anti-β-actin antibody (lower panel). (*d*) Dose-dependent effects of EGF on Parkin expression. Cell lysate was extracted from SW48 or HT29 cells 16 hr after the treatment with various concentrations of EGF (0, 10 and 100 ng/ml). Immunoblotting was performed using anti-Parkin antibody (upper panel) or anti-β-actin antibody (lower panel).

Quantitative real-time reverse transcription polymerase chain reaction

For the RT reaction, total RNA was reverse-transcribed into cDNA using the Superscript III first strand synthesis system (Invitrogen).[23] The oligonucleotide primers used in this study are shown in Supplemental Table I. PCR amplification was performed using Takara Ex Taq DNA polymerase (Takara, Tokyo, Japan). Quantification of gene expression was performed by quantitative real-time RT-PCR using a 7300 Real-Time PCR system (PE Applied Biosystems, Foster City, CA). To assess the quantity of isolated RNA, as well as the efficiency of cDNA synthesis, target cDNAs were normalized to the endogenous mRNA levels of the housekeeping reference gene, *18s ribosomal RNA (18s rRNA)*.[23] For simplicity, the expression levels of the target gene were expressed relative to those of the control specimen.

Detection and subcloning of alternatively spliced Parkin

The oligonucleotide primers for *Parkin* were designed to amplify the whole coding sequences of human *Parkin* gene shown in Supplemental Table I. All PCR products were analyzed by electrophoresis in 1.2% agarose gels stained with ethidium bromide. Subcloning of purified DNA was performed by inserting the cDNA fragment into the BamHI-EcoRI sites of pcDNA3-*Myc*.[24]

Immunoblotting analysis

Protein samples were separated by sodium dodecyl sulfate-polyacrylamide gel electrophoresis 10% (w/v) polyacrylamide gels and subjected to immunoblotting analysis as described previously.[25] Polyclonal antibodies against human Parkin and Akt were purchased from Chemicon International (CA) and Cell Signaling Technology (Danvers, MA), respectively. Monoclonal antibodies against cyclin E (E-4), c-Myc (9E10) and β-actin were purchased from Santa Cruz Biotechnology (Santa Cruz, CA) and Sigma Chemical, respectively.

Patients and tissue specimens

Colon cancer tissue specimens were obtained from 43 patients treated between 2001 and 2004, at Kyoto University Hospital, as defined by TNM classification criteria.[26] Selection of patients enrolled in this study was based on the availability of a sufficient amount of tissue for analyses. The patients included 30 men and 13 women, with a mean ± SD age of 65 ± 11.9 years (range, 36–82 years). All patients were treated by surgical resection of the involved segment of the colon. No prospective adjuvant chemotherapy was performed initially in all cases. Tissue specimens were frozen immediately in liquid nitrogen for RNA preparation, and were also fixed in 10% formalin, embedded in paraffin and subjected to histologic analyses. The study was approved by the

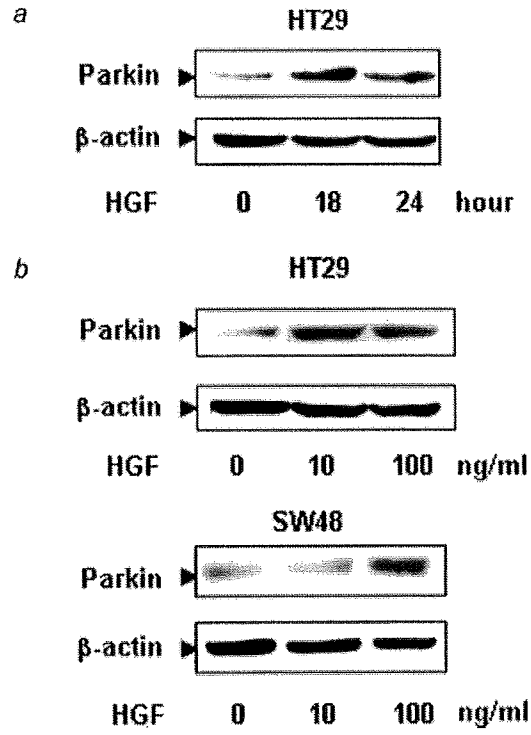

FIGURE 2 – HGF induces Parkin expression in human colon cells. (*a*) Time course of changes in Parkin protein expression. HT29 cells were harvested before (0 hr) and 18 and 24 hr after HGF (10 ng/ml) stimulation. (*b*) Dose-dependent effects of HGF on Parkin protein expression in colon cells. Cell lysate from HT29 or SW48 cells treated with HGF at the indicated concentration were subjected to immunoblotting using anti-Parkin (upper panel) or anti-β-actin (lower panel).

Kyoto University Graduate School and Faculty of Medicine Ethics Committee, and informed consent was obtained from all patients.

Results

Growth factor signaling induced Parkin expression in human colon cells

To gain insight into the role of Parkin in regulation of the cell cycle, we first examined *Parkin* gene expression in association with growth factor stimulation in cultured colon cells. First, we examined the effect of EGF on the expression of *Parkin* transcripts in several human colon cell lines. In unstimulated cells, only a trace amount of *Parkin* transcript was detected. In contrast, treatment of cells with EGF induced substantial *Parkin* expression (Fig. 1*a*). Quantitative RT-PCR analyses revealed that endogenous *Parkin* expression in both HT29 and SW48 cells markedly increased after EGF treatment, peaking 6 hr after treatment, whereas expression of the internal control *18s rRNA* transcripts was unchanged (Fig. 1*b*). Immunoblotting analysis using a specific antibody against human Parkin revealed that EGF induced time-dependent upregulation of Parkin protein in both cell lines, peaking 16 hr after treatment (Fig. 1*c*). Further, EGF stimulation induced a dose-dependent increase in Parkin expression (Fig. 1*d*). To examine whether growth factor stimulation generally enhances Parkin expression in human colon cells, we further analyzed Parkin expression in cells treated with hepatocyte growth factor (HGF). Parkin protein levels were markedly upregulated after treatment with HGF (Fig. 2*a*). Immunoblotting analyses revealed that HGF treatment induced a dose-dependent increase in Parkin expression with a maximum level obtained with 10 ng/ml in HT29 cells and 100 ng/ml in SW48 cells (Fig. 2*b*). Taken together, these findings suggested that endogenous Parkin expression is induced in response to growth factor stimulation in human colon cells.

EGF-induced Parkin expression was mediated by the Akt signaling pathway

The finding that EGF induced Parkin expression in colon cells led us to examine whether Parkin expression is mediated in a PI(3)K-Akt- or mitogen-activated protein kinase (MAPK)-dependent manner, because both of these pathways contribute to the expression and regulation of various genes downstream of EGF signaling.[27] First, we examined EGF-mediated Parkin expression in the presence of either a PI(3)K-Akt- or MAPK-inhibitor. Pretreatment with the MEK-inhibitor PD98059 had little effect on the expression of Parkin after EGF stimulation (Fig. 3*a*, upper panel). In contrast, the PI(3)K inhibitor wortmannin significantly attenuated EGF-mediated Parkin upregulation in HT29 cells (Fig. 3*a*, lower panel), suggesting that EGF-induced Parkin expression is mainly regulated by the PI(3)K-Akt-dependent signaling pathway. To further clarify whether Akt is involved in EGF-mediated Parkin expression, we examined the effects of the wild-type or dominant-negative form of Akt on Parkin expression. Quantitative RT-PCR analyses revealed that endogenous *Parkin* transcription was upregulated in colonic cells expressing wild-type *Akt* (Fig. 3*b*). Similarly, Parkin protein expression levels were significantly upregulated in the cells with wild-type *Akt* expression (Fig. 3*c*). In contrast, EGF-induced Parkin protein expression was almost completely abolished by co-production of the dominant-negative form of *Akt* (Fig. 3*d*). Taken together, these findings suggest that the EGF-mediated induction of Parkin expression in human colon cells is mainly achieved through the PI(3)K-Akt-signaling pathway.

Parkin induced proteolytic degradation of cyclin E protein in colon cells

To determine whether growth factor-mediated Parkin expression is involved in cell cycle regulation in colonic epithelial cells, we examined the expression levels of cyclin E protein in association with Parkin expression, because cyclin E is a putative substrate of Parkin-mediated proteasomal degradation in neurons.[7] Immunoblotting analyses revealed that cyclin E protein expression in HT29 cells increased in response to EGF treatment, and peaked 18 hr after stimulation. At 20 hr after EGF stimulation, when EGF-mediated Parkin protein expression was at its peak, the expression levels of cyclin E protein were substantially reduced (Fig. 4*a*). Scanning densitometry analysis using the LAS-3000 imaging system (FujiFilm, Tokyo, Japan) revealed a more than 2-fold increase in the relative amount of Parkin after EGF stimulation. To examine whether Parkin degrades cyclin E in colon cells, HT29 cells were transfected with expression plasmid encoding wild-type *Parkin* or defective *Parkin* lacking E3 activity.[2] We first confirmed that the expression of the wild-type *Parkin* resulted in little change in the *cyclin E* mRNA expression levels in HT29 cells (Fig. 4*b*). In contrast, immunoblotting analyses revealed that expression levels of endogenous cyclin E protein were significantly reduced in the presence of wild-type *Parkin*, whereas defective *Parkin* had no effect on the expression levels of cyclin E protein (Fig. 4*c*). We also confirmed that the Parkin-mediated reduction of cyclin E protein expression was reversed by treatment with a proteasome inhibitor (Fig. 4*d*). Similarly, the downregulation of cyclin E protein in association with EGF-mediated Parkin expression was suppressed in cells treated with a proteasome inhibitor (Fig. 4*e*). Immunoprecipitation assay revealed that the pretreatment of cells expressing *Parkin* with the proteosome inhibitor MG132 accelerated the ubiquitinaiton of cyclin E in these cells when compared with control cells, suggesting that cyclin E becomes a target of Parkin E3 ubiquitin ligase in colonic cells. (Supplemental Fig. 1). To clarify whether the reduction of cyclin E protein levels in the late phase of EGF stimulation was due to the upregulated Parkin protein, we knocked down the endogenous Parkin protein by transfecting a *Parkin*-specific siRNA and

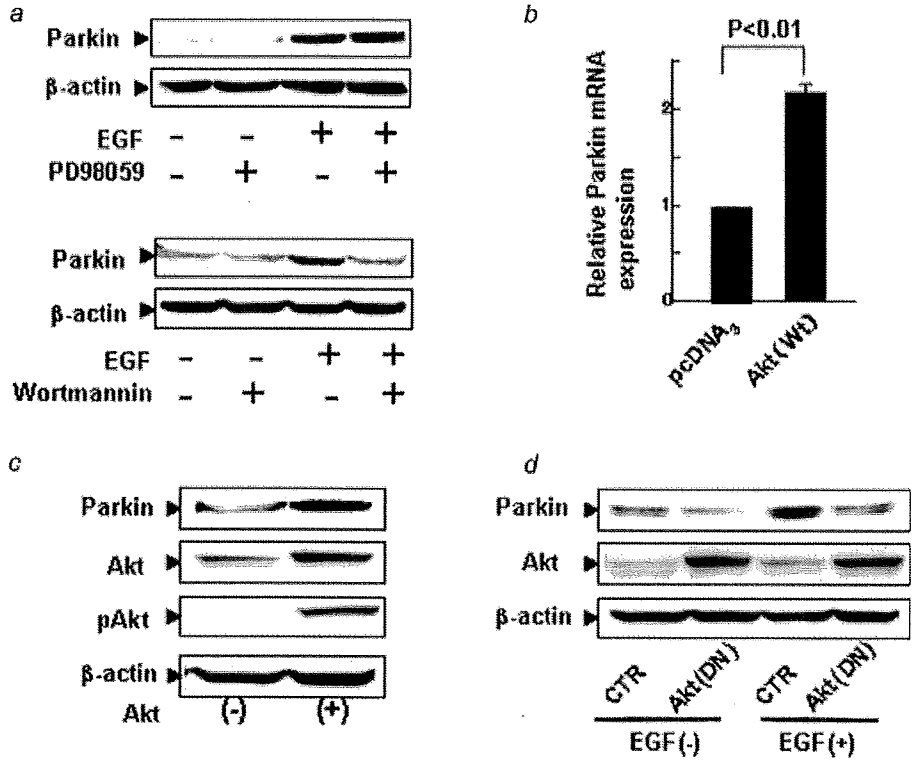

FIGURE 3 – EGF-mediated Parkin expression is induced via the Akt-signaling pathway. (*a*) Effects of the MEK-inhibitor PD98059 or Akt-inhibitor wortmannin on EGF-mediated Parkin expression. HT29 cells were treated with PD98059 (10 μM) or wortmannin (1 μM) for 30 min, and further subjected to EGF (100 ng/ml) stimulation for 18 hr. Cell lysates were probed with anti-Parkin (upper panel) or anti-β-actin (lower panel) antibodies. (*b*,*c*) HT29 cells were transfected with plasmid for the expression of wild-type human Akt [Akt(+)] or with a control vector [Akt(−)]. After 18 hr, lysates of the transfected cells were subjected to quantitative RT-PCR analyses (*b*) or immunoblotting (*c*) with anti-Parkin (upper panel), anti-Akt (Akt; upper middle panel), anti-phospho Akt (lower middle panel), or anti-β-actin (lower panel) antibodies. (*d*) Expression plasmids encoding a dominant-negative form of human *Akt* (DN) or a control vector (CTR) were transfected into HT29 cells and then treated with EGF (100 ng/ml) for 18 hr. Each sample was harvested and the extracted cell lysates were probed with anti-Parkin (upper panel), anti-Akt (Akt; middle panel) or anti-β-actin (lower panel) antibodies.

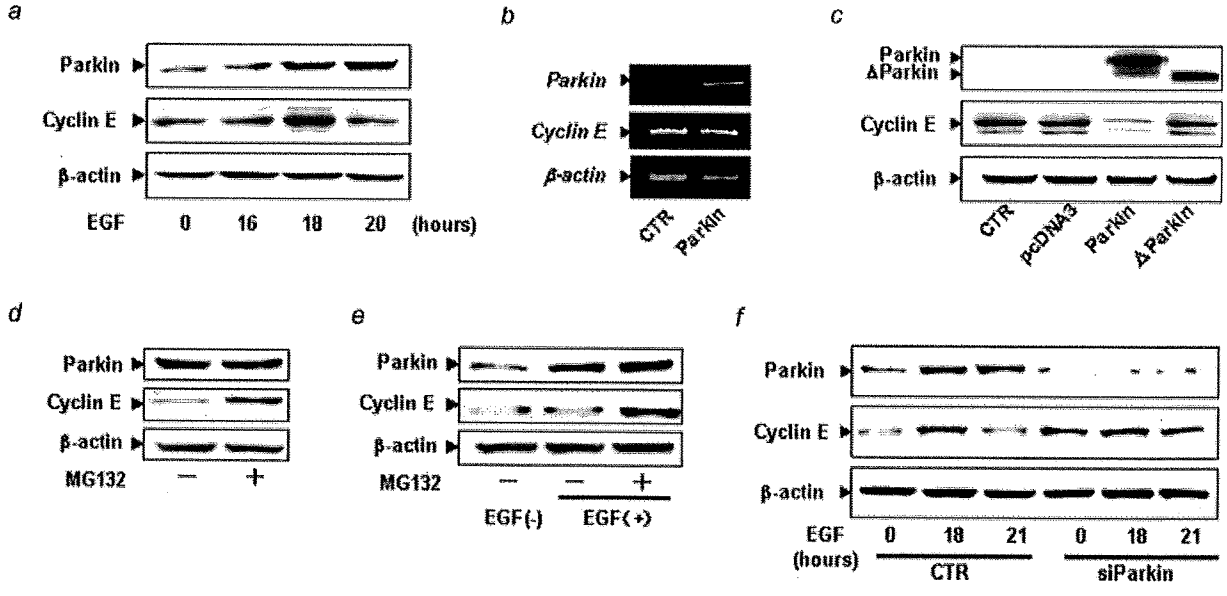

FIGURE 4